Designing Eight-port Antenna Array for Multi-Band MIMO Applications in 5G Smartphones

Zainab Faydhe Al-Azzawi, Rusul Khalid AbdulSattar, Muhannad Y. Muhsin, Mohammed Abdulrazzaq Azeez, Ali J. Salim, and Jawad K. Ali

University of Technology – Iraq, Bahdad, Iraq

https://doi.org/10.26636/jtit.2023.4.1297

Abstract — This article introduces a dual-functional low-profile compact multiple input multiple output (MIMO) antenna array for multi-band communication in 5G smartphones. The proposed eight elements of the antenna array form two different 4×4 MIMO systems. The first four elements are placed at the four mobile corners and operate in a single band of 3.445–3.885 GHz for 5G n77 and n78 applications. The other system, in which four antennas are positioned in the middle of the terminal board, supports two wide bands of 1.684–2.300 GHz and 4.432–5.638 for n2, n3, n39, n65, n66, n79, and WLAN applications. The second iteration of a modified Peano-type fractal geometry served as the design foundation for the proposed antenna element. The system's ground plane design is based on self-isolated and spatial diversity methods. The single-band MIMO system's isolation is better than 23 dB. In the dual-band MIMO system that is based on self-isolation, isolation equals approximately 16 dB in the higher band and 10 dB in the lower band. To evaluate performance, radiation-related and total antenna efficiencies, scattering parameters and gains were investigated. Additionally, ECCs have been considered to evaluate MIMO performance. According to the results, such design constitutes a valuable option for MIMO applications in 5G smartphones.

Keywords — 5G communication, compact MIMO antenna, decoupling techniques, fractal geometry, multi-band antenna

1. Introduction

The constantly increasing data transmission rates and the advent of smart services motivate researchers to develop wireless communication techniques. This leads to the need of an antenna system that can simultaneously operate with different frequencies, providing high data rates, good quality of service, and very low latency [1], [2]. The 5G technology and the Internet of Things (IoT) are recognized as the key trends capable of transforming education, industry, healthcare, and other public areas in the future [3].

The MIMO antenna technology is utilized for 5G mobile terminals to enhance spectrum efficiency and channel capacity [4], [5]. However, an increase in the number of antennas creates integration issues due to the constrained space available in mobile devices [6], [7]. Many techniques have been used to deal with this problem, including the multimode decoupling method [8] and the hybrid decoupling method (neutralization line and ground slot) [9]. Nevertheless, antenna efficiency was significantly reduced because of additional isolation-related components.

The self-isolated approach has been revealed to provide high isolation and antenna efficiency [10], [11]. However, such antenna systems operate in a single band only. As a result, developing a small, multi-band MIMO antenna with good performance and a high isolation rate has become a significant challenge.

A compact dual-functional antenna array is presented in this study for use in multi-band MIMO applications in mobile devices supporting 5G. Adequate isolation is accomplished without inserting any decoupling structures. Besides, the proposed MIMO antenna array is capable of achieving a good antenna efficiency and MIMO performance. CST Microwave Studio software has been relied upon to analyze the proposed design.

2. Proposed Antenna Array

The design of an eight-element dual MIMO antenna array for 5G handset applications is shown in Fig. 1. The antenna array comprises two different 4×4 MIMO systems. The four antennas (ant. 1–4) in the corners of the main PCB are relied upon to build a MIMO system which can operate in a single 3.445–3.885 GHz band, as part of the 5G n77 and n78 NR (new radio) bands. The other four MIMO elements (ant. 5–8) are placed in the middle of the PCB and support wide bands of 1.684–2.300 GHz for n2, n3, n39, n65, n66 4.432–5.638 GHz for n79, and 5.15-5.63 GHz WLAN.

All eight antenna elements are located on the top layer made of a 0.8 mm thick double-sided FR4 substrate with a relative permittivity of 4.3 and a loss tangent of 0.02, as shown in Fig. 1a. The thickness of the conductive layer is 35 µm. The system's circuit board has the size of 150×75 mm – a standard dimension for mobile phones. The ground bottom layer enhances the antenna's impedance matching and bandwidth, as shown in Fig. 1b. However, in the proposed design, the ground layer is slightly modified to achieve two different 4×4 MIMO systems. Figure 2 presents the design of a single compact monopole antenna element with its dimensions being

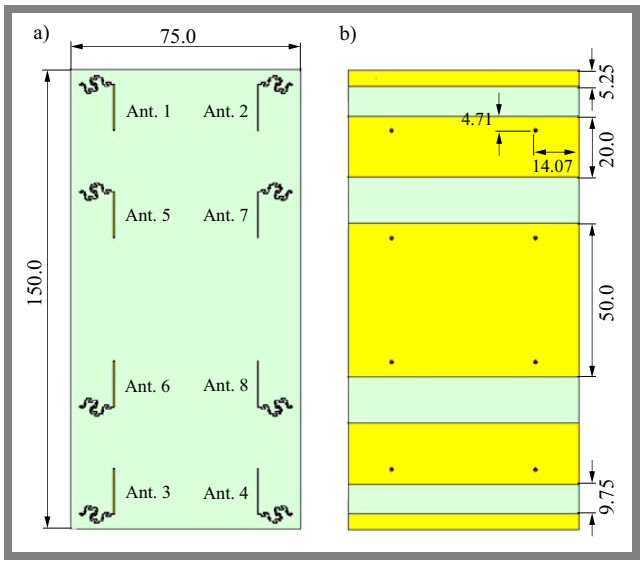

Fig. 1. Proposed MIMO antenna array: a) top view and b) back view.

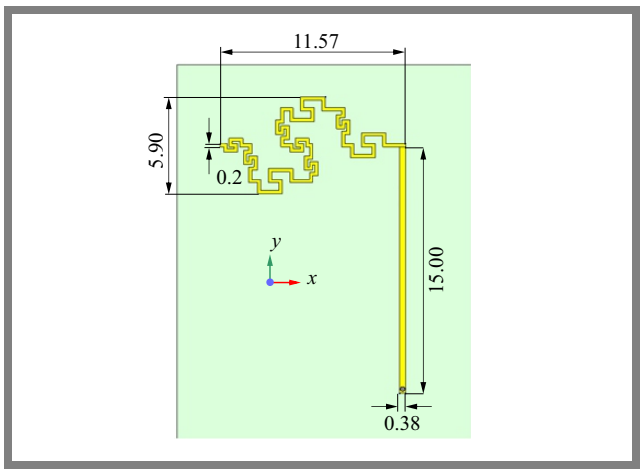

Fig. 2. Details of a single antenna element.

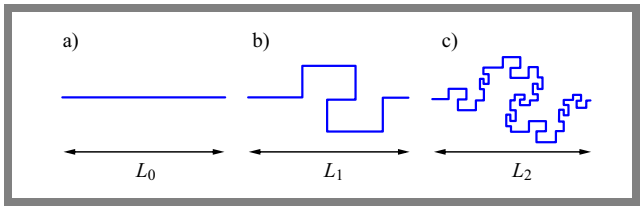

Fig. 3. The process of generating a modified Peano pre-fractal curve.

based on the second iteration of a modified Peano-type fractal geometry [12]. The process of generating a modified Peano pre-fractal curve is shown in Fig. 3.

The proposed fractal geometry is combined with a 50 Ω transmission line. RF signal is fed from a coax connector to the hole in the ground layer.

3. Performance Analysis

Figure 4 presents the results of S-parameter simulations for the proposed single-band, four-element MIMO antenna. One may notice that the desired single operating band of 3.445–3.885 GHz for 5G n77 and n78 bands applications is achieved with an acceptable impedance matching of less than –6 dB, meaning that a 3:1 voltage standing wave ratio (VSWR) has been achieved, as shown in Fig. 4a. As illustrated in Fig. 4b, decent isolation better than 23 dB is achieved by applying the self-isolated and spatial diversity methodologies, where the four MIMO antennas are placed at the corners of the PCB. The transmission coefficients are better than: S_{12} –23 dB, S_{13} –30 dB, S_{14} –37 dB (diagonal distance), S_{15} –26 dB, and S_{16} –35 dB.

Figure 5 shows the S-parameters of the dual band MIMO antenna design proposed. As shown in Fig. 5a, the operating range of 1.684–2.300 GHz for n2, n3, n39, n65, and n66

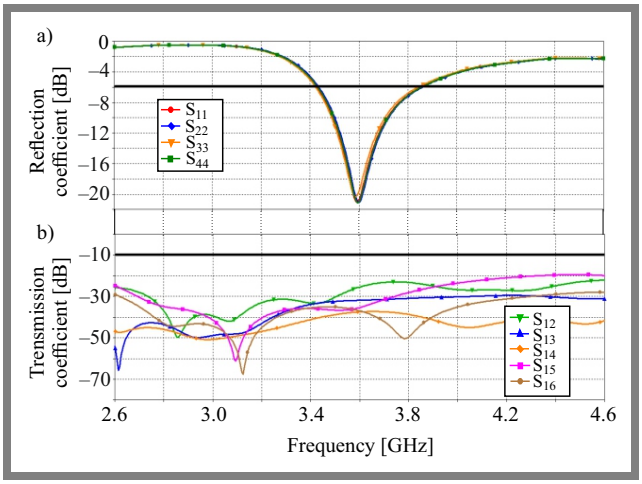

Fig. 4. S-parameters of the single band 4×4 MIMO antenna system: a) reflection coefficients and b) transmitting coefficients.

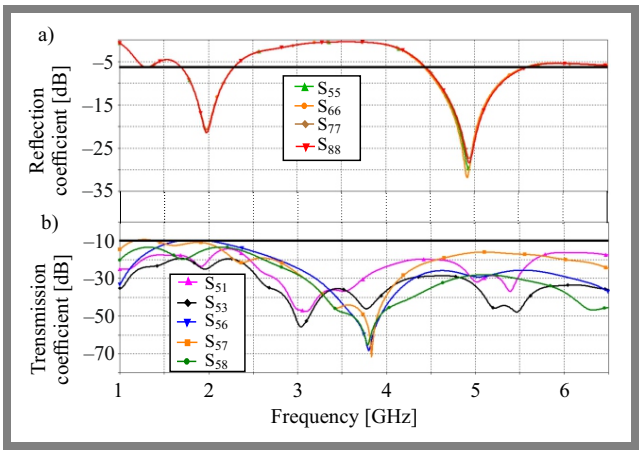

Fig. 5. S-parameters of the dual-band 4×4 MIMO antenna system: a) reflection coefficients and b) transmitting coefficients.

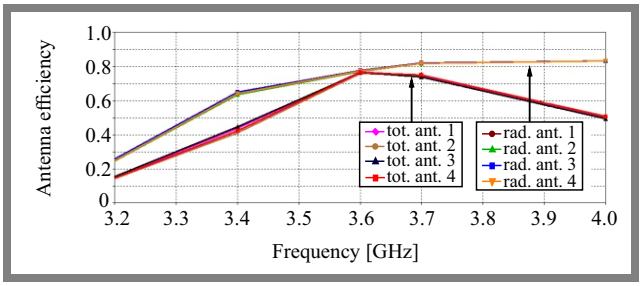

Fig. 6. Antenna efficiency of the single-band MIMO system.

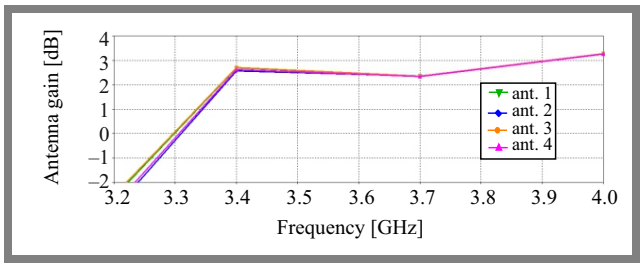

Fig. 7. Antenna gain of the single-band MIMO system.

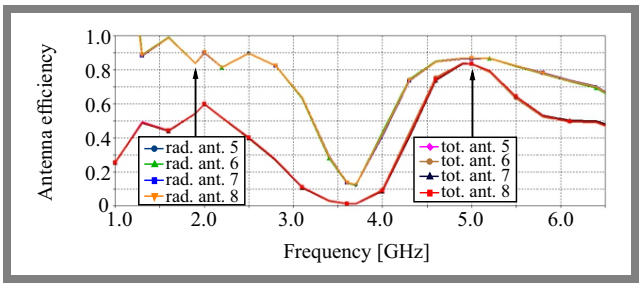

Fig. 8. Antenna efficiency of the dual-band MIMO system.

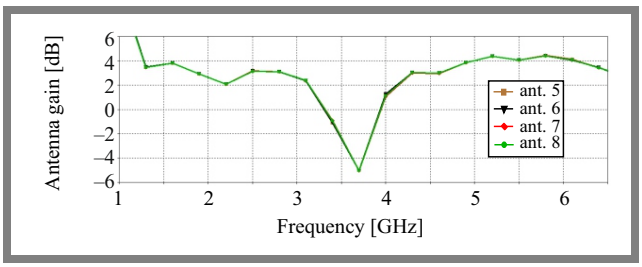

Fig. 9. Antenna gain of the dual-band MIMO system.

bands, and 4.432–5.638 GHz for n79 and 5.15–5.63 GHz for WLAN bands, works with an impedance matching score of less than –6 dB (3:1 VSWR). From Fig. 5b, suitable isolation of better than 16 dB in the higher band and acceptable isolation better than 10 dB in the lower band is attained using the self-isolated method, i.e., without inserting any decoupling parameters or/and deploying any isolation techniques, where the four MIMO antennas are located closely to each other, in the middle of the mobile phone's PCB. Only the essential transmission coefficients of the lower band are introduced, which are all better than the accepted level of –10 dB. These are as follows: the $S_{51} \approx -14$ dB, $S_{53} \approx -19$ dB, $S_{56} \approx -10$ dB, $S_{57} \approx -10$ dB, and $S_{58} \approx -13$ dB. In contrast, the transmission coefficients of the higher band are as follows: $S_{51} \approx -20$ dB, $S_{53} \approx -29$ dB, $S_{56} \approx -26$ dB, $S_{57} \approx -16$ dB, and $S_{58} \approx -28$ dB.

Figure 6 illustrates the efficiencies of the single-band four MIMO antennas setup. As illustrated, radiation antenna efficiency and total antenna efficiency levels that are acceptable for mobile phone applications are obtained. The radiation and total antenna efficiencies are between 67–82% and 50–76%, respectively. As presented in Fig. 7, good antenna gains are obtained, where the maximum gain in the working band is almost 2.6 dB. The efficiencies of the four antennas of the dual-band MIMO antenna system are shown in Fig. 8. Decent radiation and total antenna efficiencies are attained, remaining between 81–90% and 47–60%, for the lower band. For the higher band, the scores of between 79–87% and 56–84% are obtained. High antenna gains can be also observed in Fig. 9, with the maximum gain that can be reached in the lower operating band equaling approximately 3.5 dB, and approximately 4.3 dB in the higher operating band.

For clarity and due to the similarity of results, one-sided antennas (ant. 1, 3, 5, and ant. 6) are considered. Figure 10 presents two-dimensional radiation patterns at the working bands, while Fig. 11 depicts, for comparison, three-dimensional radiation patterns. As shown in the pictures, each antenna element has a maximum gain direction that differs from the maximum gain orientations of the other antennas, suggesting decent pattern diversity characteristics. Furthermore, each antenna's radiation pattern covers both sides of the mobile device PCB board. As a result, the proposed MIMO antenna systems achieve the expected level of radiation coverage.

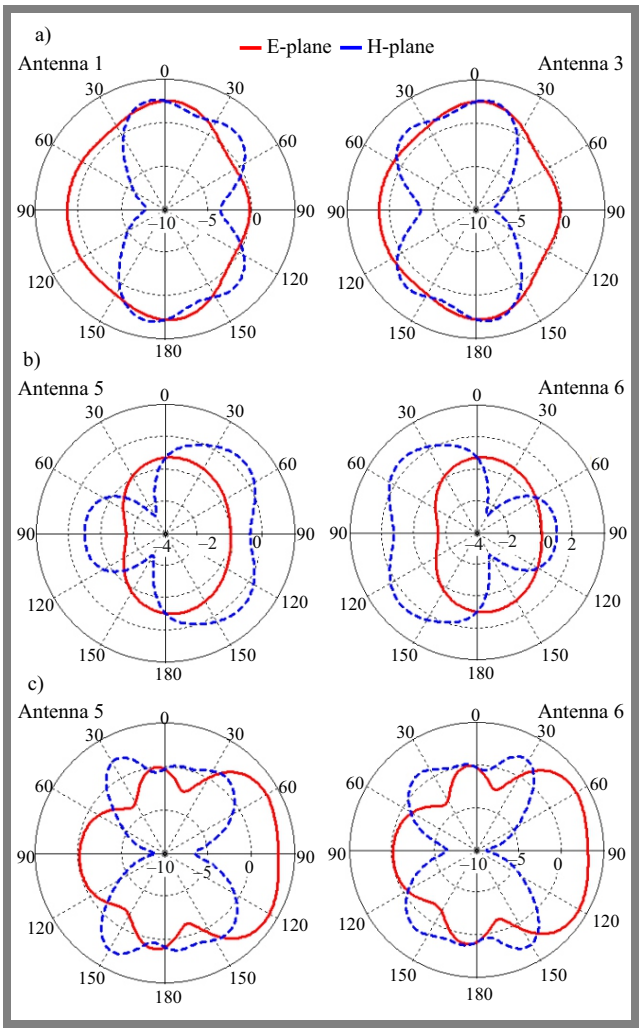

Fig. 10. Two dimensional-antenna radiation patterns at: a) 3.6 GHz, b) 2 GHz, and c) 5 GHz.

3.1. Performance of MIMO Array

The envelope correlation coefficient (ECC) is a recognized metric used to assess functionality of a MIMO antenna system [13], [14], showing the correlation or isolation of the multipath communication channels [15]. The ECCs can be

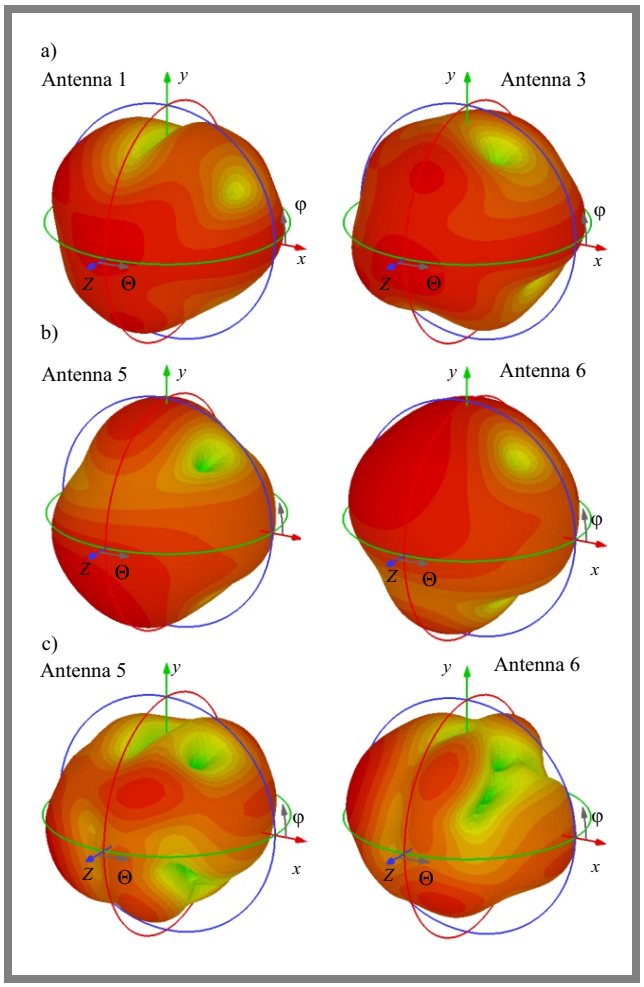

Fig. 11. Three-dimensional antenna radiation patterns at: a) 3.6 GHz, b) 2 GHz, and c) 5 GHz.

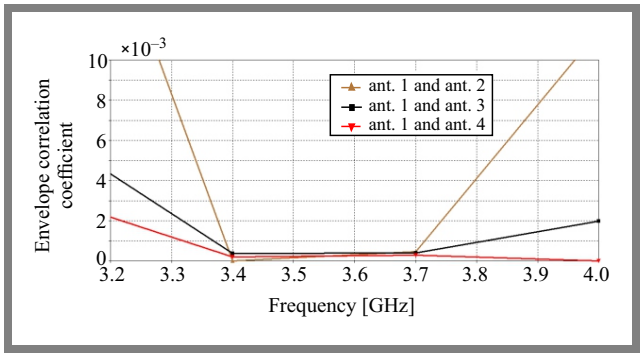

Fig. 12. ECCs of the proposed single-band MIMO antenna system.

calculated based on far-field radiations and/or S-parameters data of the antenna system. Here, Eq. (1) is used to calculate the ECCs based on far-field radiations [16].

$$\rho_e = \frac{\left| \iint\limits_{4\pi} \left[\overrightarrow{F_1}(\theta,\phi)^* \, \overrightarrow{F_2}(\theta,\phi)\right] \mathrm{d}\,\Omega \right|^2}{\iint\limits_{4\pi} \left|\overrightarrow{F_1}(\theta,\phi)\right|^2 \mathrm{d}\,\Omega \iint\limits_{4\pi} \left|\overrightarrow{F_2}(\theta,\phi)\right|^2 \mathrm{d}\,\Omega}, \qquad (1)$$

where $\overrightarrow{F_1}(\theta,\phi)$ denotes the three-dimensional far-field radiation pattern and Ω indicates the solid angle. An ECCs calculation based on the far field radiations of the single-band 4-element MIMO antenna system is sketched in Fig. 12. Values lower than 0.007 in the desired band are obtained, which is considerably below the accepted criterion according to which ECCs should be less than 0.5 in the MIMO systems. As far as a dual-band MIMO antenna system is concerned, as

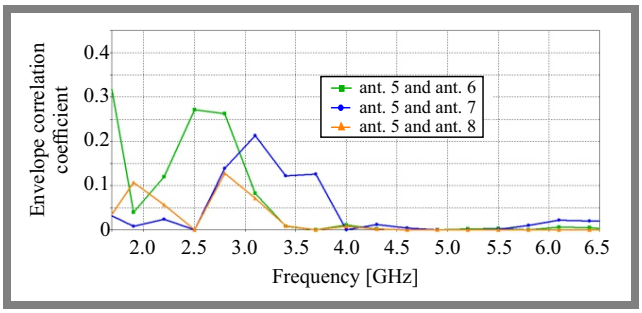

Fig. 13. ECCs of the proposed dual-band MIMO system.

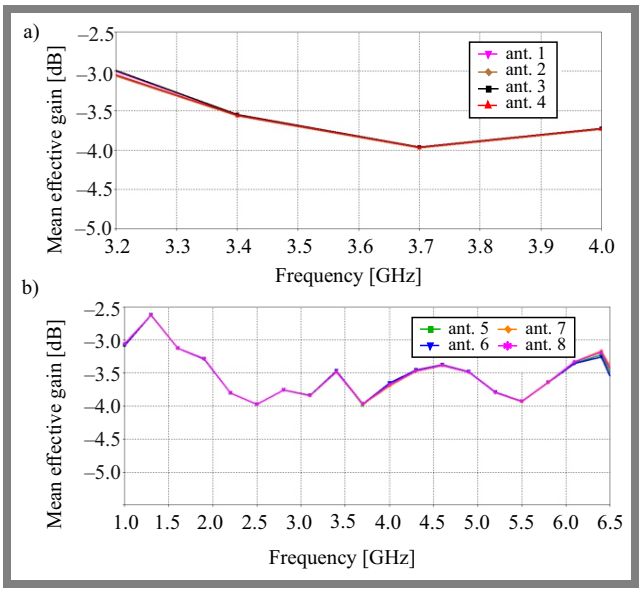

Fig. 14. MEG of the proposed: a) single-band system and b) dual-band system.

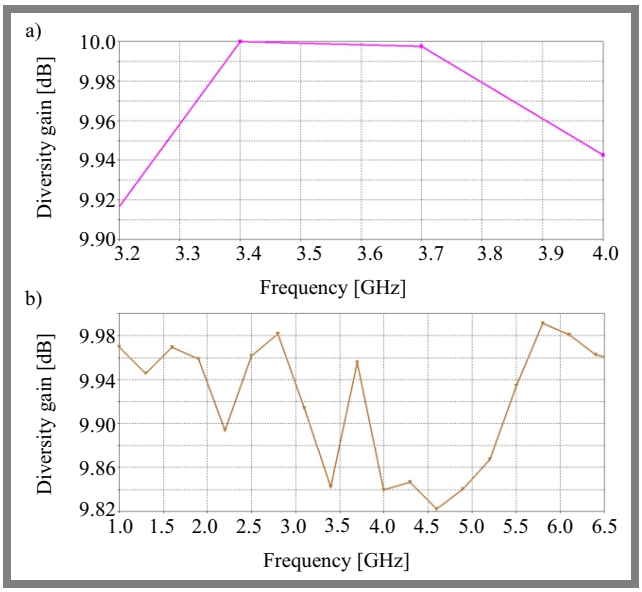

Fig. 15. Diversity gain: a) single-band system and b) dual-band system.

shown in Fig. 13, all the ECCs are lower than 0.317 within the lower working band, while the ECCs of the higher band are below 0.009. Thus, the proposed four-element MIMO antenna offers outstanding diversity performance due to its low ECC values.

One of the effective performance criteria for MIMO systems is the mean effective gain (MEG), defined as the ratio between the mean received power of the antenna and the total mean incident power [17]. MEG can be calculated using Taga's [18] formula:

$$MEG = \int_0^{2\pi}\int_0^{\pi}\left[\frac{XPR}{1+XPR}\,G_\theta(\theta,\varphi)\,P_\theta(\theta,\varphi) + \frac{1}{1+XPR}\,G_\varphi(\theta,\varphi)\,P_\varphi(\theta,\varphi)\right]\sin\theta\,\mathrm{d}\theta\,\mathrm{d}\varphi\,. \quad (2)$$

The cross-polarization power ratio (XPR) is the mean incident power ratio of vertically and horizontally polarized waves. P_θ and P_φ represent the theta and phi components of the normalized angular power density functions of the incoming plane waves, respectively. In contrast, G_θ and G_φ represent the antenna gain components. It is worth noting that the MEGs of the MIMO antennas should be close to equal to ensure good MIMO system diversity performance and system power balancing [19].

Figure 14 illustrates the MEG of the proposed single-band and dual-band MIMO antenna systems. The MEGs for all antennas of the proposed single-band and dual-band antenna systems are stable within the operational bands. Furthermore, in the MIMO system, the MEGs approximately satisfy the equality criteria applicable to antenna elements.

The diversity gain of the proposed single-band and dual-band MIMO antenna systems can be estimated with the use of a formula relative to the correlation coefficient G_{DG} [20], [21], such as:

$$G_{DG} = 10 \times \sqrt{1-|\rho|^2}\,, \quad (3)$$

High-diversity gain performance of the single-band and dual-band MIMO antenna system is shown in Fig. 15. It is better than 9.96 dB in the single-band antenna system and better than 9.82 dB in the dual-band antenna system.

4. Comparison with Other Works

Table 1 compares the performance of the proposed single-band and dual-band MIMO antenna systems with that of other recent MIMO antenna systems developed for 5G mobile terminals. As shown, the proposed solution offers a compact size antenna element, expected isolation, and adequate total antenna efficiencies thanks to employing spatial diversity and self-isolated methodology for the single-band antenna system and self-isolated technique for the dual-band antenna system. Therefore, no antenna efficiency losses are caused by other isolation elements and/or decoupling techniques.

5. Conclusions

This article presents and discusses an eight-port dual-functional MIMO antenna array for 5G mid-band MIMO applications for mobile devices. The antenna miniaturization with multi-band capability is achieved using the modified Peano-type fractal geometry space-filling feature and its self-similarity property. The design contains two four-element MIMO antennas working in different bands to serve various 5G mobile phone applications. By adopting the spatial and self-isolated techniques, suitable isolation is attained. Therefore, it is not necessary to use matching circuits, decoupling components, or re-optimizing the antenna's construction, which would increase system complexity and degrade its efficiency. An antenna element may function simultaneously as a radiated and isolated component, as it offers suitable self-isolated features. The modified Peano-type fractal geometry exhibits the ability to realize the self-isolated attribute of the antenna's components. It is evident from simulation results that the two proposed MIMO antenna systems are an attractive option when it comes to using them in mobile communication equipment.

References

[1] N.O. Parchin *et al.*, "An Efficient Antenna System with Improved Radiation for Multi-standard/Multi-mode 5G Cellular Communications", *Scientific Reports*, vol. 13, art. no. 4179, 2023 (https://doi.org/10.1038/s41598-023-31407-z).

[2] H. Zou *et al.*, "Dual-functional MIMO Antenna Array with High Isolation for 5G/WLAN Applications in Smartphones", *IEEE Access*, vol. 7, pp. 167470–167480, 2019, (https://doi.org/10.1109/ACCESS.2019.2953311).

[3] W.M. Abdulkawi, M.A. Alqaisei, A.F.A. Sheta, and I. Elshafiey, "New Compact Antenna Array for MIMO Internet of Things Applications", *Micromachines*, vol. 13, no. 9, 2022 (https://doi.org/10.3390/mi13091481).

[4] M.Y. Muhsin, A.J. Salim, and J.K. Ali, "Compact MIMO Antenna Designs Based on Hybrid Fractal Geometry for 5G Smartphone Applications", *Progress in Electromagnetics Research C*, vol. 118, pp. 247–262, 2022 (https://doi.org/10.2528/PIERC22012808).

[5] S.H. Kiani *et al.*, "Multiple Elements MIMO Antenna System with Broadband Operation for 5th Generation Smart Phones", *IEEE Access*, vol. 10, pp. 38446–38457, 2022 (https://doi.org/10.1109/ACCESS.2022.3165049).

[6] J. Cai, J. Zhang, S. Xi, J. Huang, and G. Liu, "A Wideband Eight-element Antenna with High Isolation for 5G New-Radio Applications", *Applied Sciences*, vol. 13, art. no. 137, 2022 (https://doi.org/10.3390/app13010137).

[7] R.M. Asif, A. Aziz, M.N. Akhtar, M. Amjad, and M.A. Khan, "Synthesis and Characterization of Tb Doped Ni–Zn nano Ferrites as Substrate Material for Dual-band MIMO Antenna", *Physica B: Condensed Matter*, vol. 653, art. no. 414658, 2023 (https://doi.org/10.1016/j.physb.2023.414658).

[8] H. Xu, H. Zhou, S. Gao, H. Wang, and Y. Cheng, "Multimode Decoupling Technique with Independent Tuning Characteristic for Mobile Terminals", *IEEE Transactions on Antennas and Propagation*, vol. 65, no. 12, pp. 6739–6751, 2017 (https://doi.org/10.1109/TAP.2017.2754445).

[9] W. Jiang, B. Liu, Y. Cui, and W. Hu, "High-isolation Eight-element MIMO Array for 5G Smartphone Applications", *IEEE Access*, vol. 7, pp. 34104–34112, 2019 (https://doi.org/10.1109/ACCESS.2019.2904647).

[10] M.Y. Muhsin, A.J. Salim, and J.K. Ali, "Compact Self-isolated MIMO Antenna System for 5G Mobile Terminals", *Computer Systems Science*

Tab. 1. Comparison of proposed antenna features with other recent works.

Ref.	Bandwidth [GHz]	Total efficiency [%]	Isolation [dB]	PCB size [mm × mm]	Antenna element size [mm × mm]	MIMO order	Isolation technique
[22]	3.3–3.6	42–75	>13	75 × 155	28.8 × 1	8 × 8	Balanced mode excitation
[23]	3.4–3.8 4.6–4.8	>50	>15	67 × 138	2-arm structure 13.7 and 16 arms long for 1st set, and 12.8 and 17 for others	4 × 4	Space diversity and pattern diversity
[24]	1.88–1.92 2.3–2.62	40–55 50–70	> 10	68.8 × 136	14 × 15	8 × 8	Pattern diversity
[25]	3.3–3.6	>48.6	>10	77 × 153	12 × 12	4 × 4	Characteristic mode
[26]	3.3–5 3.3-4.2	>45	>10	145 × 76	26 × 2.5 28.5 × 2.5	4 × 4 8 × 8	Self-isolated
[10]	3.4–3.6	56–66	>15	75 × 150	9.57 × 5.99	8 × 8	Self-isolated
[4]	1.66–2.30 4.8–5 5.150–5.925	57–60 78–83 60-82	>12.4 >14.8 >14.8	75 × 150	11.47 × 7.19	4 × 4	Self-isolated
	1.83–2.21 4.8–5 5.150–5.925	46–56 81-82 57-80	>11 >17 >17	75 × 150	11.47 × 7.19	8 × 8	Self-isolated
This paper	3.445–3.885	50-76	>23	75 × 150	11.57 × 5.90	4 × 4	Spatial diversity and self-isolated
	1.684-2.300 4.432-5.638	47-60 56-84	>10 >16		11.57 × 5.90	4 × 4	Self-isolated

and Engineering, vol. 42, no. 3, pp. 919–934, 2022 (https://doi.org/10.32604/csse.2022.023102).

[11] A. Zhao and Z. Ren, "Multiple-input and Multiple-output Antenna System with Self-isolated Antenna Element for Fifth-generation Mobile Terminals", *Microwave and Optical Technology Letters*, vol. 61, no. 1, pp. 20–27, 2019 (https://doi.org/10.1002/mop.31515).

[12] A.J. Salim and J.K. Ali, "Design of Internal Dual Band Printed Monopole Antenna Based on Peano-type Fractal Geometry for WLAN USB Dongle", *PIERS Proceedings*, pp. 1268–1272, 2011 (https://www.piers.org/pierspublications/PIERS2011SuzhouProceedings04.pdf).

[13] M.Y. Muhsin, A.J. Salim, and J.K. Ali, "An Eight-element MIMO Antenna System for 5G Mobile Handsets", in: *2021 International Symposium on Networks, Computers and Communications (ISNCC)*, Dubai, UAE, 2021 (https://doi.org/10.1109/ISNCC52172.2021.9615663).

[14] A.K. Sidhu and J.S. Sivia, "Design of a Novel 5G MIMO Antenna with its DGP Optimization Using PSOGSA", *International Journal of Electronics*, 2022 (https://doi.org/10.1080/00207217.2022.2148288).

[15] M.Y. Muhsin, A.J. Salim, and J.K. Ali, "An Eight-element Multi-band MIMO Antenna System for 5G Mobile Terminals", *AIP Conference Proceedings*, vol. 2651, no. 1, 2023 (https://doi.org/10.1063/5.0105773).

[16] S. Chouhan, D.K. Panda, M. Gupta, and S. Singhal, "Multiport MIMO Antennas with Mutual Coupling Reduction Techniques for Modern Wireless Transreceive Operations: A Review", *International Journal of RF and Microwave Computer-Aided Engineering*, vol. 28, no. 2, art. no. e21189, 2018 (https://doi.org/10.1002/mmce.21189).

[17] A.A. Glazunov, A.F. Molisch, and F. Tufvesson, "Mean Effective Gain of Antennas in a Wireless Channel", *IET Microwaves, Antennas & Propagation*, vol. 3, no. 2, pp. 214–227, 2009 (https://doi.org/10.1049/iet-map:20080041).

[18] T. Taga, "Analysis for Mean Effective Gain of Mobile Antennas in Land Mobile Radio Environments", *IEEE Transactions on Vehicular Technology*, vol. 39, no. 2, pp. 117–131, 1990 (https://doi.org/10.1109/25.54228).

[19] M. Abdullah, S.H. Kiani, and A. Iqbal, "Eight Element Multiple-input Multiple-output (MIMO) Antenna for 5G Mobile Applications", *IEEE Access*, vol. 7, pp. 134488–134495, 2019 (https://doi.org/10.1109/ACCESS.2019.2941908).

[20] L. Malviya, R.K. Panigrahi, and M.V. Kartikeyan, "MIMO Antennas with Diversity and Mutual Coupling Reduction Techniques: a Review", *International Journal of Microwave and Wireless Technologies*, vol. 9, no. 8, 1763–1780, 2017 (https://doi.org/10.1017/S1759078717000538).

[21] M.S. Sharawi, "Printed Multi-band MIMO Antenna Systems and their Performance Metrics", *IEEE Antennas and Propagation Magazine*, vol. 55, no. 5, pp. 218–232, 2013 (https://doi.org/10.1109/MAP.2013.6735522).

[22] D. Huang, Z. Du, and Y. Wang, "Slot Antenna Array for Fifth Generation Metal Frame Mobile Phone Applications", *International Journal of RF and Microwave Computer-Aided Engineering*, vol. 29, no. 9, art. no. e21841, 2019 (https://doi.org/10.1002/mmce.21841).

[23] M.A. Jamshed *et al.*, "Dual Band and Dual Diversity Four-element MIMO Dipole for 5G Handsets", *Sensors*, vol. 21, no. 3, art. no. 767, 2021 (https://doi.org/10.3390/s21030767).

[24] Z. Qin, G. Wen, M. Zhang, and J. Wang, "Printed Eight-element MIMO System for Compact and Thin 5G Mobile Handest", *Electronics*

Letters, vol. 52, no. 6, pp. 416–418, 2016 (https://doi.org/10.1049/el.2015.3960).

[25] L. Sun, H. Feng, Y. Li, and Z. Zhang, "Tightly Arranged Orthogonal Mode Antenna for 5G MIMO Mobile Terminal", *Microwave and Optical Technology Letters*, vol. 60, no. 7, pp. 1751–1756, 2018 (https://doi.org/10.1002/mop.31240).

[26] L. Guo, Z. Liu, H. Liu, D. Huang, and Z. Du, "Wideband Eight-element Antenna for 5G Metal Frame Mobile Phone Applications", *International Journal of RF and Microwave Computer-Aided Engineering*, vol. 30, no. 12, art. no. e22442, 2020 (https://doi.org/10.1002/mmce.22442).

Zainab Faydhe Al-Azzawi, M.Sc.
Department of Communication Engineering
https://orcid.org/0000-0002-1627-751X
E-mail: zainab.f.mohammad@uotechnology.edu.iq
University of Technology – Iraq, Bahdad, Iraq
https://uotechnology.edu.iq

Rusul Khalid AbdulSattar, M.Sc.
Department of Electrical Engineering
https://orcid.org/0000-0002-9019-3840
E-mail: rusul.k.abdulsattar@uotechnology.edu.iq
University of Technology – Iraq, Bahdad, Iraq
https://uotechnology.edu.iq

Muhannad Y. Muhsin, Ph.D.
Department of Electrical Engineering
https://orcid.org/0000-0003-3937-4467
E-mail: muhannad.y.muhsin@uotechnology.edu.iq
University of Technology – Iraq, Bahdad, Iraq
https://uotechnology.edu.iq

Mohammed Abdulrazzaq Azeez, Ph.D.
Department of Communication Engineering
E-mail: mohammed.a.azeez@uotechnology.edu.iq
University of Technology – Iraq, Bahdad, Iraq
https://uotechnology.edu.iq

Ali J. Salim, Ph.D.
Department of Communication Engineering
https://orcid.org/0000-0003-3185-5063
E-mail: alijsalim@gmail.com
University of Technology – Iraq, Bahdad, Iraq
https://uotechnology.edu.iq

Jawad K. Ali, Prof.
Department of Communication Engineering
https://orcid.org/0000-0002-6900-6844
E-mail: jawad.k.ali@uotechnology.edu.iq
University of Technology – Iraq, Bahdad, Iraq
https://uotechnology.edu.iq